

Supporting information

Finite Element formulation:

The sequential coupling algorithm in COMSOL was utilized to simulate the fluid-thermal interactions. In this iterative coupling procedure, each domain (thermal and fluid) is solved sequentially and the governing matrix equations for the two domains are solved separately. The solver iterates between each physics field (thermal and fluid) until loads converge. The equations and the boundary conditions involved in laser induced heating of a solvated oligomer are discussed below.

Heat transfer:

The elevation of the temperature in the fluid, T, due to laser absorption is described by the following set of equations:¹

$$\rho C_p \frac{\partial T}{\partial t} + \nabla \cdot (-k \nabla T) = Q - \rho C_p \mathbf{u} \cdot \nabla T \quad \text{Equation 1}$$

$$Q(x, y, z) = Q_0 (1 - R_c) \cdot \frac{A_c}{\pi \sigma_x \sigma_y} e^{-\left[\frac{(x-x_0)^2}{2\sigma_x^2} + \frac{(y-y_0)^2}{2\sigma_y^2}\right]} \cdot e^{-A_c z} \quad \text{Equation 2}$$

In the above equations, x, y and z refer to the Cartesian coordinates, k is the thermal conductivity, T is the temperature, u is the velocity of the fluid σ_x is Gaussian pulse along x direction with standard deviation ~0.5 •m, σ_y is Gaussian pulse along y direction with standard deviation 0.75 µm, Q_0 is laser power~3.15 W, R_c is the reflection coefficient (0.05), A_c is the absorption coefficient (for water it is 0.5 [1/cm]), t is time and the temporal pulse width is around 100 ns.

Fluid dynamics:

In the fluid domain, we need to first consider mass and momentum balances as shown below:¹

$$\rho \frac{\partial \mathbf{u}}{\partial t} + \nabla \cdot [p \mathbf{I} - \eta (\nabla \mathbf{u} + (\nabla \mathbf{u})^T)] = \mathbf{F} - \rho (\mathbf{u} \cdot \nabla) \mathbf{u} \quad \text{Equation 3}$$

where the body force is $\mathbf{F} = -\rho(T)gh$ *i.e.* the force arising from gravity.

In the above equations, ρ is the fluid density, F is the body force, p is the pressure, and η is the viscosity, which contributes to viscous dissipation of energy.

Coupling conditions:

The coupling between the heat transfer and fluid dynamics domain was carried out *via* two dependent variables namely temperature and velocity. The increase in temperature gradient helps diffuse heat and also changes the density of water. Due to buoyancy effect arising from a change in water density with respect to temperature, there is a corresponding flow and also heat dissipation within water due to convection.

Density variation at the various temperatures:

Table S1: Average density of various systems studied during this work.

Temperature (K)	Heating Cycle		Cooling Cycle
	Average Density of Systems (g/cc)	Average Density of Systems (g/cc)	
278	1.02	-	
285	0.98	0.97	
290	0.97	0.97	
295	0.96	0.96	
298	0.96	0.96	
300	0.96	0.96	
302	0.95	0.96	
304	0.95	0.96	
306	0.96	0.96	
310	0.95	0.95	
315	0.95	0.95	

Initial equilibration:

Initial equilibration was performed by running the system at 278 K for 20 ns. Apart from equilibration of density, temperature, and system energy (attained with a few hundreds of picoseconds); one must also check the equilibration of the structure of the macromolecule. To probe that equilibration is adequate at this temperature, we evaluate the root mean squared deviation (RMSD) of the atoms in the oligomer and find that at 278 the RMSD does indeed fluctuate around an average value (~ 40 Angstrom) with a negligible drift after a trajectory interval of ~ 5 ns. Thus, while the equilibration of density, temperature and system energy are attained within 1 ns, the structural equilibration takes slightly longer time. At 278 K, the oligomer is in a coil-like-configuration. The open coil structures correspond to the backbone C-C-C-C dihedral angle being in the trans configuration (lowest energy conformation on the C-C-C-C potential energy surface) and it takes about 5 ns for the oligomer to relax to its equilibrium state.

When we heat the polymer, more states on the potential energy surface including the higher energy conformations of cis become available for the polymer to explore because of temperature increase resulting in increased thermal motions of the molecules. The rotational barriers of 5 kcal/mol to translocate from trans to cis conformations become easier due to increased thermal energy provided to the system. There are couple of state points at 60 and -60 which conform to the gauche+ and gauche- conformations and only 0.5 kcal/mol above the global minima of trans (180). These states become available and the polymer backbone dihedral samples these state points with increasing temperatures. Hence, during the heating cycles all the state points on the potential energy surface are available due to temperature effects. When the polymer collapses above the LCST, the dihedral populations are primarily in the local minima conformation of 60, -60 and high energy cis conformations. There are equally represented trans conformations too. Thus, it is a mixed population based on all the conformations unlike the open coil form of PNIPAM below LCST (<285 K), which primarily has trans conformations.

During the ultrafast cooling cycle, the probability of overcoming the 5 kcal/mol barrier becomes less with decreasing temperatures as the thermal motions are reduced due to lowered temperatures. The efficiency of sampling the various states in the potential energy surface is not the same as the heating cycle. The conformations of the backbone dihedral in the local minima of gauche+ and gauche- are unable to overcome this 5 kcal/mol barrier as the temperatures are reduced. This is a typical manifestation of the non-equilibrium effect. Hence longer time scales are required at a particular temperature to overcome these barriers, a manifestation of hysteresis owing to non-equilibrium effects.

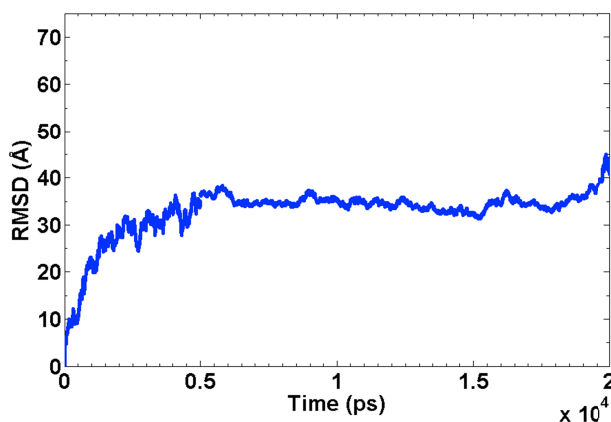


Figure S1: Temporal evolution of the root mean squared deviation of the backbone atoms of the PNIPAM oligomer at 278 K

Velocity Autocorrelation functions:

It should be noted that the long-time tails in the VACF can lead to numerical uncertainties if the long-time tails are not accounted for properly. Apart from averaging over numerous statistical samples to accurately sample the tail of a long

time correlation, we must perform a long time simulation for each velocity autocorrelation.

In our manuscript, for each of the correlation function, we have taken care to choose the correct array size of the velocity correlation function. This dictates the sampling of the long-time tails in VACF. Figure R2 shows the VACF of carbon atom of CH1 group of backbone of PNIPAM polymer chain for four different correlation lengths (512, 1024, 2048 and 4096). Moreover, we have also taken care to choose a large number of configurations ($\sim 100,000$) and sampled frequently (0.1 fs) to ensure accurate statistics.

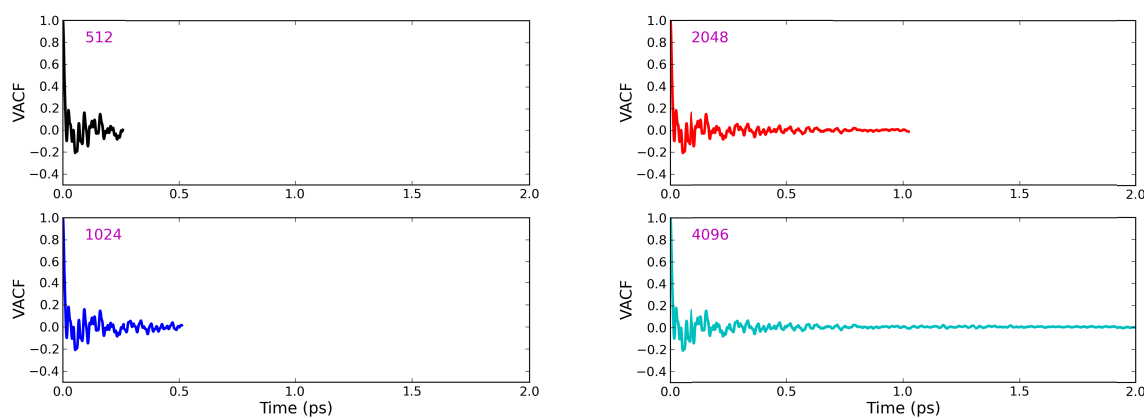


Figure S2: VACF of carbon atom of CH1 group of backbone of PNIPAM polymer chain for four different correlation lengths (512, 1024, 2048 and 4096).

Figure S2 clearly shows that the long-time tails in the VACF are dependent on the correlation length. For VACF array lengths of 512 and 1024, the long time tails are not adequately accounted for whereas for 2048 and 4096 array lengths adequately account for the long-time tails. The corresponding vibrational spectra for these VACFs are shown in Figure S3. We observe that the vibrational density of states converge when proper array length (2048 and higher) is chosen. For each of the vibrational spectra shown in the manuscript, we had taken care to sample adequate configurations and choose the correct correlation length to ensure that the results are numerically consistent.

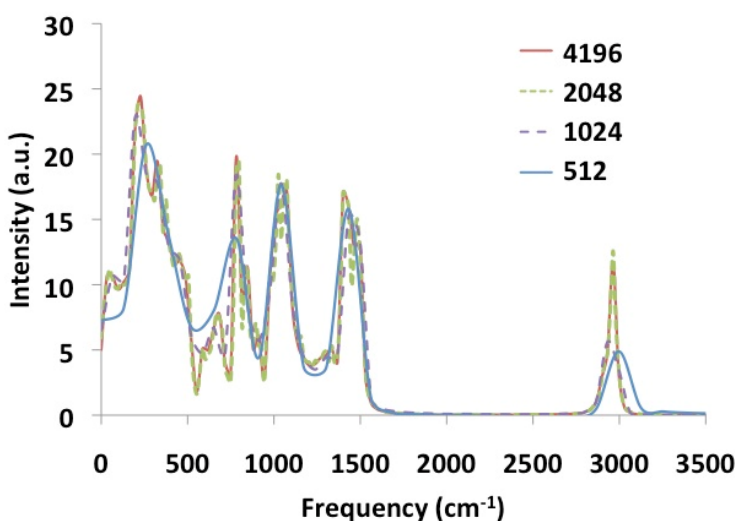


Figure S3: VACF of carbon atom of CH1 group of backbone of PNIPAM polymer chain.

The non-monotonic trends in the vibrational density of states observed during the ultrafast heating-cooling cycles are in fact a manifestation of the non-equilibrium effects. The insufficient relaxation time scales during the heating-cooling cycles lead to fluctuations in the polymer configurations, which are captured in the vibrational spectra.

Potential energy surface scan:

We have performed a potential energy scan using both electronic structure calculations and empirical PCFF force field used in our MD simulations. At the lowest simulated temperature *i.e.* 278 K, the trans states at 180°/-180° in Fig. S4 correspond to the global minima for the potential energy surface for the backbone dihedral rotation (Fig. S5 and S6). For electronic structure calculations, a relaxed potential energy dihedral scan in increments of 15 degree for the C-C-C-C backbone dihedral for a dimer- two units of NIPAM- at M062X/cc-pvdz level of theory and basis set using the SMD solvation model for implicit water solvent at 278 K was performed using Gaussian 09. The potential energy surface for the dihedral rotation revealed a minimum at -180 and 180 corresponding to the trans configuration. Similarly, high-energy states were seen for the dimer at torsion angle of -120°, 120°, and 0°. The difference in the high energetic regions and low energetic regions was found to be around 5 kcal/mol. This confirms indeed that the coil state corresponds to mostly an all trans configuration as seen by the low energy regions at -180° and 180°. A small fraction of the dihedral population assumes a gauche+ conformation (+60°) (Fig. S4), which is expected since it is about 0.5 kcal/mol higher than the global minimum (Fig S5). Similar results are obtained from the PES scan using PCFF force field for polymer in explicit water (Fig. S6). This analysis confirms that the initial configuration after 20 ns of MD simulation run at 278 K does correspond to the equilibrium coil state.

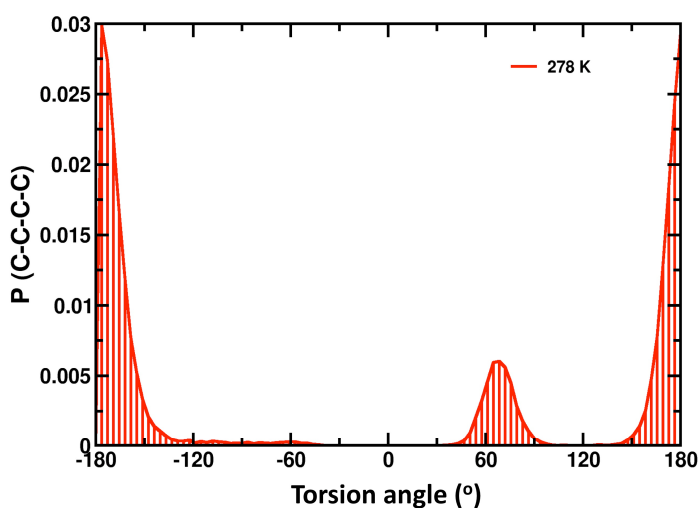


Figure S4: The population distribution for the backbone dihedral in PNIPAM at 278 K during the heating and cooling cycles obtained from MD simulations. As seen from the distribution, the proportion of trans vs. gauche states at 278 K is similar to that expected from the torsional minima at this temperature (see Figs. S5 and S6).

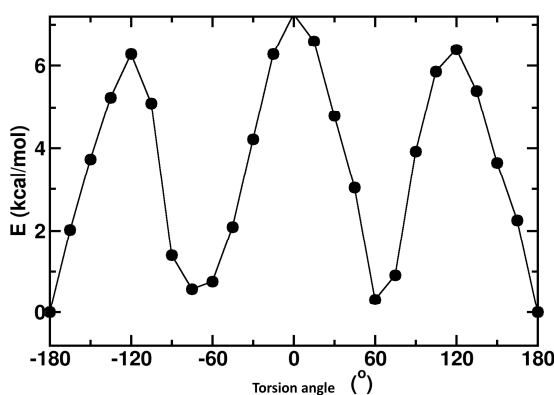


Figure S5: Potential energy surface (PES) scan as a function of the torsion angle from electronic structure calculations of the NIPAM dimer dihedral in implicit solvent water using SMD solvation model and M062X/ccpvdz basis set at 278 K.

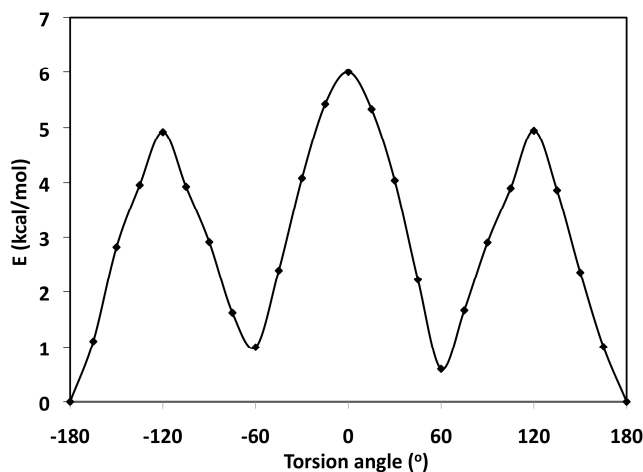


Figure S6: Potential energy surface (PES) scan as a function of the torsion angle of the NIPAM dimer dihedral in explicit water and PCFF force field at 278 K.

Reference:

-
- (1) Nikrityuk, P. A. *Computational Thermo-Fluid Dynamics: In Materials Science and Engineering*; John Wiley & Sons, 2011.
 - (2) Gaussian 09, Revision D 01, M. J. Frisch, G. W. Trucks, H. B. Schlegel, et al., Gaussian, Inc., Wallingford CT, 2009.